Available online at www.sciencedirect.com
SCIENCE DIRECT®
Catalysis Today 91–92 (2004) 181–184
CATALYSIS TODAY
www.elsevier.com/locate/cattod

A study of active sites for partial oxidation on α-$Bi_2Mo_3O_{12}$ and β-$Bi_2Mo_2O_9$ catalysts using crystal structure visualization

Takehiko Ono [a,*], Kazuya Utsumi [a], Masakazu Kataoka [a], Yumo Tanaka [a], Fumio Noguchi [b]

[a] *Department of Environmental Science and Technology, Faculty of Engineering, Shinshu University, 4-17-1 Wakasato, Nagano 380-8551, Japan*
[b] *Department of Applied Chemistry, Faculty of Engineering, Saitama University, 255 Shimo-ookawa, Saitama 338-8570, Japan*

Abstract

The unit cells of α-$Bi_2Mo_3O_{12}$, β-$Bi_2Mo_2O_9$, and γ(H)-Bi_2MoO_6 are visualized by the crystal structure application. These oxides have twin Mo tetrahedra structures. The visualization clarified that Mo ions of twin Mo tetrahedra and some Bi ions with these Bi–Mo oxides lie on the same plane. It is proposed that the active sites for selective oxidation is linked with these structures exposed on the surface.

Keywords: Unit cells of Bi–Mo oxides; Crystal structure visualization; Selectivity in propene oxidation; Dispcrystal

1. Introduction

It has been well known that α-$Bi_2Mo_3O_{12}$ and β-$Bi_2Mo_2O_9$ catalysts exhibited 95% of selectivity for partial oxidation of propene to acrolein (e.g., [1]). It was reported that pure γ(L)-Bi_2MoO_6, i.e., pure koechlinite, has no selectivity for partial oxidation but the mixtures of γ(L)-Bi_2MoO_6 + MoO_3 or γ(L)-Bi_2MoO_6 + α-$Bi_2Mo_3O_{12}$ exhibited high selectivity [2]. Buttrey et al. reported that a connection between the fluorite structure and bismuth molybdates has been established in selective oxidation catalysis [3] and that the actual structure of the γ phase surface present during catalysis should be re-examined by the structural refinement of γ(L) and γ(H) phases [4]. Anderson et al. reported in a quantum chemical study that the $Bi_2Mo_3O_{20}^{12-}$ cluster model chosen for the catalysis mechanism study has all the cations nearly in a plane and is bulk superimposable [5]. α-$Bi_2Mo_3O_{12}$ catalyst has three Mo tetrahedra α_1, α_2, and α_3 [6]. We have previously reported that the oxide ions of α-$Bi_2Mo_3O_{12}$ were exchanged with ^{18}O via oxidation of olefins using $^{18}O_2$ and that the oxide ions which are responsible for oxidation reactions were determined by Raman spectrum analysis [7,8]. In this work, the unit cell of α-$Bi_2Mo_3O_{12}$, β-$Bi_2Mo_2O_9$, and γ(H)-Bi_2MoO_6 are visualized by the application such as Dispcrystal, which are made by one of the authors (Noguchi). The active sites for partial oxidation and the nature of active sites, i.e., the configuration of Mo, Bi, and O in the lattice, are proposed and discussed.

2. Methods

Noguchi has developed an application Dispcrystal using space group method. Lattice constants of α-$Bi_2Mo_3O_{12}$, β-$Bi_2Mo_2O_9$, and γ(H)-Bi_2MoO_6 and the values of *x*, *y*, and *z* coordinates of all ions are given in Cifdata [4,6,9]. These give the visualization of Mo, Bi, and O ions on the display. If we omit the values of *x*, *y*, and *z* coordinates of oxygen ions, we can get the arrangement of unit cell of Mo and Bi ions without oxygen. The Dispcrystal also indicates the values of distances of Mo–O, O–O, Bi–O, and of Mo–O–Bi angles in any case. By a rotation of unit cell on the display, we can get whether the arrangements of Mo and Bi ions lie on a plane or not. The exchange of oxygen with ^{18}O using the reaction of olefins with $^{18}O_2$ were studied previously [7,8]. The results of oxygen activity with various olefins were also shown below.

3. Results and discussion

3.1. Visualization of α-$Bi_2Mo_3O_{12}$

The unit cell of α-$Bi_2Mo_3O_{12}$ crystal was visualized by Dispcrystal application as described in Section 2. Fig. 1

* Corresponding author.
E-mail address: takeono@gipwc.shinshu-u.ac.jp (T. Ono).

0920-5861/$ – see front matter © 2004 Elsevier B.V. All rights reserved.
doi:10.1016/j.cattod.2004.03.057

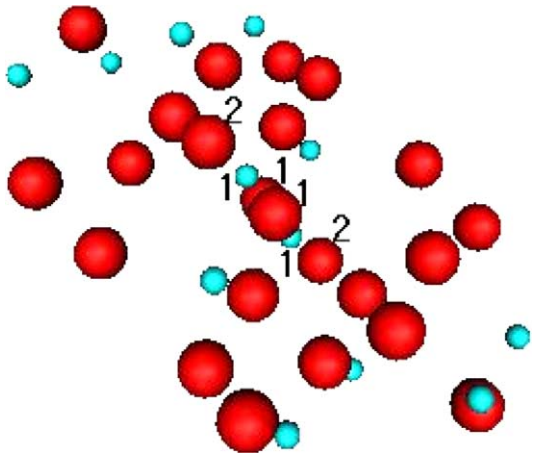

Fig. 1. Visualization of $\alpha_1\alpha_1$ twin tetrahedra (in the middle of figure) in α-$Bi_2Mo_3O_{12}$ crystal structure without oxygen. Small spheres denote Mo_1 ions. Large spheres denote Bi_1 and Bi_2 ions. Other Mo_2 and Mo_3 ions, oxygen ions, and axes are omitted here. Numerals are the position numbers of Mo and Bi reported by van den Elzen and Riek [6].

expresses three unit cells in which Mo_1 ions of α_1 tetrahedron and all Bi ions contain, while Mo_2, Mo_3 and oxygen ions are omitted. The Mo_1 tetrahedron (α_1) with oxygen ions is shown in Fig. 2a, which should be located at all Mo_1 positions in Fig. 1. Oxygen ions in Mo_1 tetrahedron were numbered as 2, 4, 5, and 10 as reported by van den Elzen and Riek [6]. The π-allyl species seem to be able to coordinate Mo_1 ions at the space between O_2–O_{10} since α_1 is extremely distorted like that. The $\alpha_1\alpha_1$ twin tetrahedra is also shown in Fig. 2b. This twin should exist at Mo_1Mo_1 position in the middle of Fig. 1. Furthermore, four Bi ions and two Mo_1 ions of $\alpha_1\alpha_1$ tetrahedra lie on the same plane as shown in Fig. 1. This was also confirmed that both angles of Mo_1–O_2–Bi and Mo_1–O_{10}–Bi are calculated as 130°. The $\alpha_1\alpha_1$ has good symmetry as shown in Fig. 2b. Similar characterization was also done with $\alpha_2\alpha_3$ twin Mo tetrahedra, which are shown in Fig. 3. Two sets of Mo_2 and Mo_3 ions of $\alpha_2\alpha_3$ also lie on the same plane with four Bi ions. The numbers of Bi ions adjacent to twin Mo tetrahedra are 2, which are less than 4 in $\alpha_1\alpha_1$. Anyway, α-$Bi_2Mo_3O_{12}$

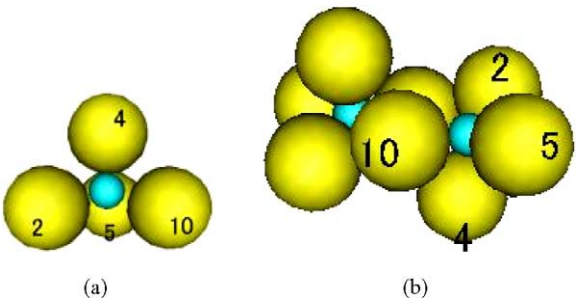

Fig. 2. Visualization of (a) α_1 tetrahedron and (b) $\alpha_1\alpha_1$ twin tetrahedra in α-$Bi_2Mo_3O_{12}$ crystal structure. Small spheres denote Mo ions and large spheres denote oxygen ions. Numerals are oxygen position numbers reported by van den Elzen and Riek [6].

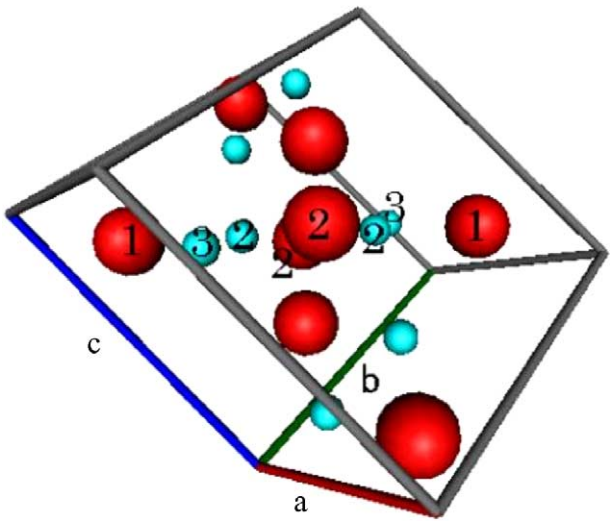

Fig. 3. Visualization of $\alpha_2\alpha_3$ twin tetrahedra and Bi ions without oxygen in α-$Bi_2Mo_3O_{12}$ crystal structure. Small spheres denote Mo_2 and Mo_3 ions and large spheres denote Bi_1 and Bi_2 ions. Mo_1 and all oxygen ions are omitted. Numerals are the position numbers of Mo and Bi as reported by van den Elzen and Riek [6]. a, b, and c denote axes.

gives $\alpha_1\alpha_1$ and $\alpha_2\alpha_3$ twin tetrahedra structures and their Mo ions are lying in a plane with some Bi ions. The hydrogen abstraction and oxygen insertion to allyl species seem to take place via oxygen of Mo tetrahedra.

3.2. *Oxygen reacted using ^{18}O tracer over α-$Bi_2Mo_3O_{12}$ catalyst*

Table 1 shows the tendency of the activity for oxygen replacement reported previously [7,8]. These were obtained from olefin oxidations using $^{18}O_2$. α-$Bi_2Mo_3O_{12}$ exhibited six Raman bands at 960, 930, 905, 856, 845, and 820 cm^{-1}. These bands are correlated to Mo–O bond lengths empirically by Wachs and coworkers [10,11]. Band shape analysis of the Raman spectra were carried out and the extents of exchange were obtained [8].

As shown in Table 1, the Mo–O species of α_1 and α_2 associated with 865 and 845 cm^{-1} were shifted preferentially for propene oxidation, while the Mo–Os of α_3 were less exchanged. Reoxidation in the case of propene oxidation seems to take place preferentially at the vacancies of Mo_1–O_5 (α_1) and Mo_2–O_9 (α_2) and those seem to be also responsible for partial oxidation. Low activity of Mo_3–O_{12}, Mo_1–O_4, and Mo_2–O_1 seems to be attributed to their stronger bonds, i.e., they are shorter bond lengths such as 1.68, 1.69, and 1.72 Å, respectively [6]. Low activity of Mo–Os of α_3 seems to be lack of Bi ions compared to $\alpha_1\alpha_1$ [8]. Similar results obtained with *trans*-but-2-ene at initial and low conversions as shown in Table 1. This seems to link with similar activity of allylic hydrogen to that of propene. However, the differences among oxygen species become smaller with an increase in exchange. With but-1-ene, any oxygen ions were well exchanged and little difference was observed among α_1–α_3,

Table 1
Tendency of active oxygen species revealed by ^{18}O exchange by the oxidations of propene, *trans*-but-2-ene, and but-1-ene using $^{18}O_2$ tracer over α-$Bi_2Mo_3O_{12}$ catalyst reported previously [7,8]

Bond species	Mo_3–O_{12}	Mo_1–O_4	Mo_2–O_1	Mo_1–O_5	Mo_2–O_9	Mo_3–O_{11}
α tetrahedra exchange activity	α_3	α_1	α_2	α_1	α_2	α_3
Propene	−−	+	+	++	++	+
trans-But-2-ene	−−	+ → ++	+	++	++	+ → ++
But-1-ene	−−	++	−−	++	++	++

(−−) less or not determined; (+) low exchange; (++) high exchange; (α) Mo tetrahedron species. Numerals of Mo and O are position numbers reported by van den Elzen and Riek [6]. Exchanges become + → ++ from low to high exchange conversions in the oxidative dehydrogenation of *trans*-but-2-ene [8].

suggesting that the dehydrogenation reaction of but-1-ene takes place at any oxygen ions. This should originate from higher activity of allylic hydrogen of but-1-ene by one order compared to propene and *trans*-but-2-ene.

According to Grasselli et al. [12–16], initial hydrogen abstraction in the oxidation of C_3H_6 involves oxygen ions associated with Bi cations and the second hydrogen abstraction is facilitated by the presence of Mo oxygen polyhedra. A rapid equilibration between σ- and π-allyl intermediates was also confirmed previously [8,12–16]. With α phase, however, oxygen ions contact to both Bi and Mo cations. The selective oxidation of olefins should take place at the sites where $\alpha_1\alpha_1$ and $\alpha_2\alpha_3$ are existed as twin tetrahedra structures and these Mo ions are lying with some Bi ions in a plane.

3.3. Visualization of β-$Bi_2Mo_2O_9$ structure

β-$Bi_2Mo_2O_9$ crystal has β_1, β_2, β_3, and β_4 Mo tetrahedra and four kinds of Bi cations [4,9]. Fig. 4 shows four sets of twin $\beta_1\beta_4$ tetrahedra and four Bi_3 ions without oxygen ions. Small spheres denote Mo ions and large spheres denote Bi ions. It is interesting that Mo_1 and Mo_4 ions and Bi_3 ions lie on the same plane. This corresponds to (1 0 1) plane of β-$Bi_2Mo_2O_9$ by adding oxygen ions. In the case of twin $\beta_2\beta_3$, Mo_2 and Mo_3 ions did not lie on the same plane with Bi_1 and Bi_2 ions although the figure is not shown. Bi_4 ions also did not lie on the same plane with Mo ions. The situation of twin $\beta_1\beta_4$ is the same as that of $\alpha_1\alpha_1$ tetrahedra of α-$Bi_2Mo_3O_{12}$. It is well known that β-$Bi_2Mo_2O_9$ catalyst has high selectivity for the partial oxidation of propene and butene [1]. The sites consisted of twin $\beta_1\beta_4$ and Bi ions on a plane seem to be responsible for partial oxidation of olefins though it is necessary that the plane exposes on the catalyst surface.

3.4. Visualization of γ(H)-Bi_2MoO_6 structure

With γ(H)-Bi_2MoO_6 catalyst, the crystal structure without oxygen is shown in Fig. 5. As reported by Buttrey et al. [4], it has γ_1, γ_2, γ_3, and γ_4 Mo tetrahedra. They exist as $\gamma_2\gamma_3$, $\gamma_4\gamma_4$, and $\gamma_1\gamma_1$, i.e., twin tetrahedra structures. Fig. 5 shows that twin $\gamma_2\gamma_3$ are present in the middle of unit cell and that they are surrounded by six Bi ions. Furthermore, these Mo

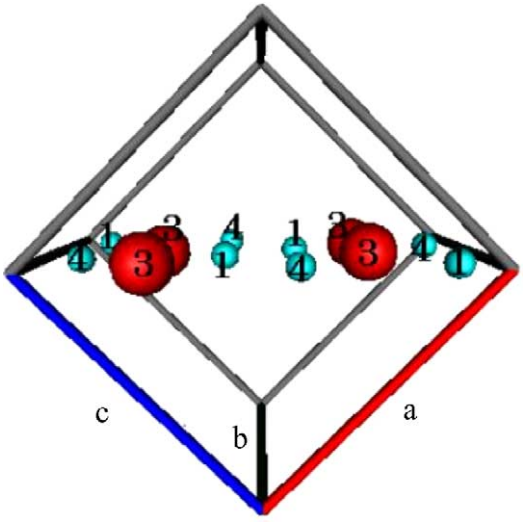

Fig. 4. Visualization of Mo_1 and Mo_4 ions of twin $\beta_1\beta_4$ and Bi_3 ions in β-$Bi_2Mo_2O_9$ crystal structure without oxygen ions. Small spheres denote Mo ions and large spheres denote Bi ions. $Mo_{2,3}$, $Bi_{1,2,4}$, and all oxygen ions are omitted. Numerals are the position numbers of Mo and Bi as reported by Buttrey et al. [4]. a, b, and c denote axes.

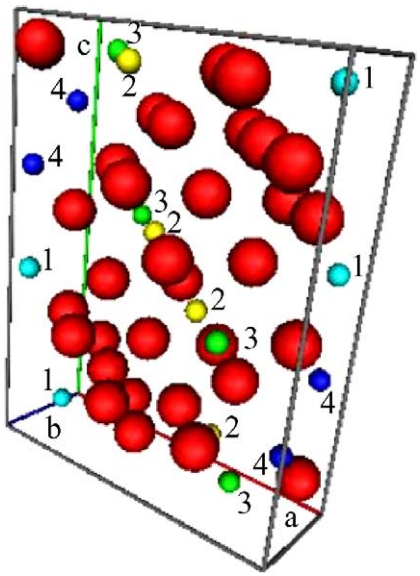

Fig. 5. Visualization of γ(H)-Bi_2MoO_6 crystal structure without oxygen ions (it is shown that two twin Mo_2 and Mo_3 ions and six Bi ions are lying in a plane). Small spheres denote Mo ions and large spheres denote Bi ions. Numerals are the position numbers of Mo and Bi as reported by Buttrey et al. [4]. a, b, and c denote axes.

and Bi ions lie on the same plane as in the case of $\beta_1\beta_4$ tetrahedra in Fig. 4. Mo ions of $\gamma_4\gamma_4$ and $\gamma_1\gamma_1$ did not lie on the plane with Bi ions though the figures are not shown. Only twin $\gamma_2\gamma_3$ are the same as those of $\beta_1\beta_4$ for β phase and $\alpha_1\alpha_1$ for α phase as described above.

Matsuura et al. have reported that pure γ(L)-Bi_2MoO_6, i.e., pure koechlinite, has no selectivity for partial oxidation [2]. Buttrey et al. have reported that actual structure of the γ phase surface present during catalysis should be re-examined since the oxygen sites coordinated only to Bi ions in γ(L) phase have very low site potentials [4]. In this work, γ(H)-Bi_2MoO_6 seems to have high selectivity in partial oxidation because it has twin Mo tetrahedra structure and Mo and Bi ions lie on the same plane. On the other hand, γ(L)-Bi_2MoO_6 consists of Mo–O, O, and Bi–O layers. Mo and oxygen exists as distorted octahedral structure [6]. The pure γ(L) phase seems to be less selective in partial oxidation because of the lack of twin Mo tetrahedral structure and lack of lying Mo ions with Bi ions on the same plane.

4. Conclusion

High selectivity seems to be linked with twin Mo tetrahedra structure and lying of their Mo and Bi ions on the same plane. The abstraction of hydrogen and insertion of oxygen seem to take place on oxygen ions of twin Mo tetrahedra. Such characteristic structure are confirmed with α-$Bi_2Mo_3O_{12}$, β-$Bi_2Mo_2O_9$, and γ(H)-Bi_2MoO_6 by computer visualization. This was supported by previous work that oxygen species of α-$Bi_2Mo_3O_{12}$ were active for selective oxidation using Raman spectra and ^{18}O tracer. The lying of Bi and Mo ions in the same plane seem to be suitable and important for redox features of Mo and Bi ions, i.e., some electrons transfer between them during the reaction. More studies will be needed for β-$Bi_2Mo_2O_9$ and γ(H)-Bi_2MoO_6 in future.

References

[1] T.D. Snyder, G.C. Hill, Catal. Rev. Sci. Eng. 31 (1989) 43, and literatures therein.
[2] I. Matsuura, R. Shut, K. Hirakawa, J. Catal. 63 (1980) 152.
[3] D.J. Buttrey, D.A. Jefferson, J.M. Thomas, Philos. Mag. A 53 (1986) 897.
[4] D.J. Buttrey, T. Vogt, U. Wildgruber, W.R. Robinson, J. Solid State Chem. 111 (1994) 118.
[5] A.B. Anderson, D.W. Ewing, Y. Kim, R.L. Grasselli, J.D. Burrington, J.F. Brazil, J. Catal. 96 (1985) 222.
[6] A.F. van den Elzen, G.D. Riek, Acta Cryst. B 29 (1973) 2433.
[7] T. Ono, N. Ogata, J. Catal. 90 (1994) 2113.
[8] T. Ono, N. Ogata, R.L. Kuczkowski, J. Catal. 175 (1998) 185.
[9] H. Chen, A.W. Sleight, J. Solid State Chem. 63 (1986) 70.
[10] F.D. Hardcastle, I.E. Wachs, J. Raman Spectrosc. 40 (1990) 683.
[11] F.D. Hardcastle, I.E. Wachs, J. Phys. Chem. 95 (1991) 10763.
[12] R.K. Grasselli, J.D. Burrington, J.F. Brazdil, Faraday Discuss. Chem. Soc. 72 (1982) 203.
[13] R.K. Grasselli, C.T. Kartisek, J.D. Burrington, J. Catal. 81 (1983) 489.
[14] R.K. Grasselli, J.D. Burrington, I&E Product Res. Dev. 23 (1984) 393.
[15] R.K. Grasselli, J.F. Brazdil, J.D. Burrington, in: Proc. 8th Int. Congr. Catal., vol. V, Berlin, 1984, p. 369.
[16] R.K. Grasselli, J. Chem. Ed. 63 (1986) 216.